Iron isotope composition of some Archean and Proterozoic iron formations

Noah Planavsky [a,b,*], Olivier J. Rouxel [b,c], Andrey Bekker [d], Axel Hofmann [e], Crispin T.S. Little [f], Timothy W. Lyons [a]

[a] *Department of Earth Sciences, University of California, Riverside, CA 92521, USA*
[b] *Department of Marine Chemistry and Geochemistry, Woods Hole Oceanographic Institute, Woods Hole, MA 02543, USA*
[c] *Department of Marine Geosciences, IFREMER, Centre de Brest, 29280 Plouzané, France*
[d] *Department of Geological Sciences, University of Manitoba, Winnipeg, MB, Canada R3T 2N2*
[e] *Department of Geology, University of Johannesburg, PO Box 524, Auckland Park 2006, Johannesburg, South Africa*
[f] *School of Earth and Environment, University of Leeds, Leeds LS2 9JT, United Kingdom*

Received 27 December 2010; accepted in revised form 31 October 2011; available online 8 December 2011

Abstract

Fe isotopes can provide new insight into redox-dependent biogeochemical processes. Precambrian iron formations (IF) are deserving targets for Fe isotope studies because they are composed predominantly of authigenic Fe phases and record a period of unprecedented iron deposition in Earth's history. We present Fe isotope data for bulk samples from 24 Archean and Proterozoic IF and eight Phanerozoic Fe oxide-rich deposits. These data reveal that many Archean and early Paleoproterozoic iron formations were a sink for isotopically heavy Fe, in contrast to later Proterozoic and Phanerozoic Fe oxide-rich rocks. The positive δ^{56}Fe values in IF are best explained by delivery of particulate ferric oxides formed in the water column to the sediment–water interface. Because IF are a net sink for isotopically heavy Fe, there must be a corresponding pool of isotopically light Fe in the sedimentary record. Earlier work suggested that Archean pyritic black shales were an important part of this light sink before 2.35 billion years ago (Ga). It is therefore likely that the persistently and anomalously low δ^{56}Fe values in shales are linked with the deposition of isotopically heavy Fe in IF in the deeper parts of basins. IF deposition produced a residual isotopically light dissolved Fe pool that was captured by pyritic Fe in shales. Local dissimilatory Fe reduction in porewater and associated diagenetic reactions resulting in pyrite and carbonate precipitation may have further enhanced Fe isotope heterogeneity in marine sediments, and an 'iron shuttle' may have transported isotopically light Fe from shelf sediments to the basin. Nevertheless, water-column processing of hydrothermally delivered Fe likely had the strongest influence on the bulk iron isotope composition of Archean and Paleoproterozoic iron formations and other marine sediments.
© 2011 Elsevier Ltd. All rights reserved.

1. INTRODUCTION

The ocean–atmosphere system was largely anoxic in the early Precambrian, which led to a Fe cycle much different than today's (Canfield, 2005; Holland, 2005; Rouxel et al., 2005). Iron would have been highly soluble in the anoxic and sulfate-poor early ocean, resulting in a period of intense Fe cycling before the rise of atmospheric oxygen and ocean oxygenation (Holland, 2005; Bekker et al., 2010). Microbial Fe oxidizers and reducers likely fueled a significant portion of this cycle; these metabolisms were probably important components of Earth's early biosphere (Hartman, 1984; Walker, 1984; Widdel et al., 1993; Konhauser et al., 2002;

Kappler et al., 2005; Crowe et al., 2008). Laterally extensive, highly Fe-rich sedimentary deposits – iron formations (IF) – are the most conspicuous evidence for substantial Fe redox cycling in the early oceans (Holland, 2005). Despite extensive research on IF, mechanisms for IF deposition and their role in the early Fe cycle remain debated (Klein, 2005; Beukes and Gutzmer, 2008; Bekker et al., 2010).

Iron isotopes allow us to trace Fe cycling and thus can improve our understanding of the mechanisms of IF deposition (Johnson et al., 2003, 2008b; Dauphas and Rouxel, 2006; Johnson and Beard, 2006; Anbar and Rouxel, 2007). Much of the utility of Fe isotopes lies with their ability to fingerprint redox processes; the largest isotope fractionations are associated with redox transformations. For example, partial microbial and abiotic ferrous oxidation produces ferric oxides enriched in heavy Fe isotopes. Isotopic fractionations induced by oxidation in closed systems and in systems where Fe removal dominates over Fe supply are well-described by a Rayleigh fractionation model (Bullen et al., 2001; Welch et al., 2003; Balci et al., 2006; Johnson et al., 2008b). The exact mechanisms of fractionation during ferrous Fe oxidation and ferric oxide precipitation remain debated (Bullen et al., 2001; Welch et al., 2003; Croal et al., 2004; Anbar et al., 2005; Beard et al., 2010), but there appears to be a maximum fractionation [Fe(III)$_{solid}$ - Fe(II)$_{aq}$] of around 1‰–3‰ at 25 °C. Experimental work suggests two-step fractionation during ferric oxide formation: an equilibrium isotope exchange between Fe(III)$_{aq}$ and Fe(II)$_{aq}$ is responsible for a 3.0‰ effect, and kinetic isotope fractionation upon precipitation of Fe(OH)3 results in ~1‰ fractionation in the opposite direction (Welch et al., 2003). Recently, Beard and others (Beard et al., 2010) experimentally determined Fe isotope fractionation between aqueous ferrous iron and goethite and found an equilibrium isotope fractionation of 1.05 ± 0.08‰ at 22 °C. These experiments indicate that the interaction of Fe(II)$_{aq}$ and goethite results in near-complete Fe isotope exchange over 30 days, involving at least four components: Fe(II)$_{aq}$, goethite, adsorbed Fe(II), and Fe(III)$_{surface}$.

Dissimilatory microbial Fe reduction (DIR) can produce large Fe isotope fractionations between Fe(III)$_{solid}$ and Fe(II)$_{aq}$ with variably depleted δ^{56}Fe values in the generated dissolved Fe (Beard et al., 1999; Icopini et al., 2004; Crosby et al., 2007). The extent of fractionation during DIR varies with the proportions of aqueous Fe(II), adsorbed Fe(II) and reactive Fe(III) on particle surfaces (Crosby et al., 2005, 2007). There are typically smaller fractionations associated with non redox-dependent processes. Siderite formation, for example, has an equilibrium fractionation factor of ~ -0.5‰ with aqueous Fe(II) (Wiesli et al., 2004). There are several recent detailed reviews covering the magnitude and mechanisms of Fe isotope fractionations (Dauphas and Rouxel, 2006; Anbar and Rouxel, 2007; Johnson et al., 2008b).

The δ^{56}Fe values of modern marine Fe sources are relatively well known. Igneous rocks have near-zero δ^{56}Fe values that cluster at 0.09‰ relative to the IRMM-14 standard (Dauphas and Rouxel, 2006; Anbar and Rouxel, 2007; Johnson et al., 2008b). Deep-sea hydrothermal vents (Severmann et al., 2004; Rouxel et al., 2008a; Bennett

et al., 2009) and shelf sediment porewaters (Severmann et al., 2006; Staubwasser et al., 2006; Homoky et al., 2009) generally have dissolved ferrous Fe with negative δ^{56}Fe values, ranging from +0.1 to −0.9 and from +0.4 to <−3, respectively. With some rare exceptions (Bergquist and Boyle, 2006; Escoube et al., 2009), fluvial systems also typically carry isotopically light dissolved Fe. Likewise, the Fe isotope composition of dissolved Fe in open and coastal seawater has been shown to range between slightly positive (+0.7‰) to negative (−1.8‰) values (Lacan et al., 2008; John and Adkins, 2010; Rouxel and Auro, 2010). Hydrothermal systems are generally considered to be the primary source of Fe to the early Precambrian ocean (Isley, 1995; Bau et al., 1997; Krapež et al., 2003), indicating there was a strong flux of dissolved Fe to bottom waters with an average δ^{56}Fe value somewhere between 0 and −0.5‰.

Since we have now a basic understanding of Fe isotope fractionation factors and the δ^{56}Fe values of different iron species entering the oceans, Fe isotope composition of marine sediments can offer insight into processes of Fe deposition, the δ^{56}Fe values of dissolved Fe in ancient oceans, and specific mechanisms of Fe cycling. Here, we present new Fe isotope data for bulk samples from 24 Archean and Proterozoic IF and eight Phanerozoic distal hydrothermal deposits for comparison.

An estimate of the average δ^{56}Fe value of IF is essential to constructing an iron isotope mass balance for the early ocean (Dauphas and Rouxel, 2006). There is typically little (<1‰) isotopic variation in Phanerozoic marine siliciclastic deposits (Beard et al., 2003; Rouxel et al., 2003) and chemically (i.e., hydrogeneous) precipitated sediments (Rouxel et al., 2003; Levasseur et al., 2004). In contrast, Archean sediments show much larger Fe isotope variations; the observed 4.5‰ range includes both positive and negative values relative to average continental crust (e.g., Rouxel et al., 2005; Johnson et al., 2008b).

A secular δ^{56}Fe trend, foremost from the sedimentary black shale record, is now widely recognized. However, the mechanisms behind this trend are still debated (Rouxel et al., 2005; Yamaguchi et al., 2005). The unmatched variability seen in Archean and early Paleoproterozoic sedimentary rocks has been linked to deposition of isotopically heavy IF, reflecting high delivery of hydrothermal Fe to a sulfur-poor anoxic deep ocean (Rouxel et al., 2005). Alternatively, this peak in Fe isotope variability may reflect a period of enhanced microbial Fe reduction when microbial sulfate reduction was limited due to the low levels of seawater sulfate and abundant Fe oxides (Johnson et al., 2008b). Additionally, Severmann et al. (2008) argued that an enhanced flux of isotopically light Fe transported from shallow-marine settings to the deep ocean might explain the observed Precambrian pattern. Shallow-to-deep Fe shuttling is suggested in redox-stratified marine basins, such as the modern Black Sea (reviewed in Lyons and Severmann, 2006) and could have relevance to the Earth's early oceans. Our new iron isotope data, when viewed in light of available facies models for IF, can help to refine our understanding of various Fe sources and sinks in Precambrian oceans.

2. ANALYTICAL METHODS

Ten to over a hundred grams of cleaned drill-core or fresh outcrop material were crushed between two plexiglass disks inside a polypropylene bag using a hydraulic press. The resulting rock chips were further cleaned using several rinses with deionized water and ultrasonification. The cleaned material was homogenized and powdered in an agate shatter-box. About 100 mg of powder were then dissolved in an ultra-pure HNO_3–HCl–HF acid mixture. Iron was purified on Bio-Rad AG1X8 anion resin, and Fe isotope ratios were determined with a Thermo-Electron Neptune multicollector inductively coupled plasma mass-spectrometer (MC-ICP-MS) following previously published methods (Rouxel et al., 2005, 2008a,b). We operated the MC-ICP-MS in either medium or high-resolution mode, and we used Ni as an internal standard for mass bias correction. Fe isotope values are reported relative to the standard IRMM-14 using the conventional delta notations (Supplementary Table 1). We measured several georeference materials, including one IF (IF-G) and one Hawaiian Basalt (BHVO-1). We obtained a $\delta^{56}Fe$ value of $0.67\permil$ for the IF-G standard, which is similar to previously reported values (Dauphas and Rouxel, 2006). Based on duplicate chemical purifications and isotope analyses, the long-term external reproducibility is $0.08\permil$ for $\delta^{56}Fe$ and $0.11\permil$ for $\delta^{57}Fe$ (2 standard deviations). Mineralogy was determined through a combination of standard petrographic techniques and X-Ray diffraction (XRD).

3. SAMPLE DETAILS

We present Fe isotope data from Si- and Fe-dominated sedimentary rocks with low levels of detrital siliciclastic and volcaniclastic material. Most of the samples in this study are Al-poor (<1 weight% Al_2O_3) and Fe-rich (>10 weight% Fe_2O_3). The Fe is present predominantly in a carbonate, silicate or oxide phases. Our sample set is composed largely of granular and banded IF, as well as ferruginous cherts that have limited spatial distribution (e.g., hydrothermal jaspers). However, we also present results for some ferruginous shales associated with IF and some cherts that contain less than 10% Fe_2O_3, since their elevated Fe/Al ratios (>5 compared to ~0.5 for average continental crust) indicate that Fe in these rocks is also predominantly of an authigenic origin.

Following Beukes and Gutzmer (2008) and Gross (1980) we group IFs into two broadly defined types: Superior-type and Algoma-type IF. Superior-type IF typically reflect deposition in close association with shelf sediments such as carbonates and shales (Beukes and Gutzmer, 2008). Even IF deposited in shelf settings, however, appear to be linked to strong hydrothermal Fe supply, albeit from distal sources (Bekker et al., 2010). Algoma-type IF, in contrast, occur in close spatial association with bimodal (mafic and felsic) volcanic rocks, basinal shales, and hydrothermal deposits. Superior-type IF commonly extend over hundreds of square kilometers; Algoma-type iron formations are typically more restricted in their aerial extent.

We have avoided samples from sequences that have experienced obvious secondary ore-forming processes (e.g., supergene Fe-enrichment). Samples with visible sign of fluid flow (extensive veining, disruption of sedimentary features, and mineral phases cross-cutting sedimentary layers) were also avoided. Given that mineral assemblages in even the best-preserved samples of Archean and early Paleoproterozoic IF have been strongly influenced by post-depositional alteration (e.g., Bekker et al., 2010), we focused on bulk (hand sample-sized) analyses rather than analysis of individual mineral separates. For instance, magnetite is a ubiquitous component of IF and, in most cases, is thought to be a late-stage diagenetic or metamorphic mineral, even in well-preserved IF like those in the Hamersley province (e.g., Tompkins and Cowan, 2001; Krapež et al., 2003). We also chose to use a bulk sample approach because one of the central goals of this work was to provide an estimate of the average Fe isotope composition of IF, rather than distinct mineral phases. Sample details and relevant references with locality information are listed in Supplementary Tables 1 and 2.

4. RESULTS

We found a wide range of $\delta^{56}Fe$ values for bulk samples of IF (Fig. 1). Archean to early Paleoproterozoic IF (ca. 3.0 to 2.45 Ga) have values ranging from $-1.53\permil$ to $1.61\permil$ (Fig. 2) with a mean of $0.4\permil$ ($n = 43$). These formations were deposited before the rise of atmospheric oxygen at ca. 2.4 Ga (Bekker et al., 2004) and are from both Algoma-type and Superior-type IF (Supplementary Table 1). There is no statistically significant difference in the data for Superior-type and Algoma-type IF (see Supplementary Table 1). However, the mean for Algoma-type IF ($\delta^{56}Fe = 0.55\permil$) is slightly higher than that for Superior-type IF ($\delta^{56}Fe = 0.29\permil$). Furthermore, the Superior-type IF contain the most negative $\delta^{56}Fe$ values (e.g., for the ca. 2.95 Ga Pongola IF). Our sample set is composed predominately of oxide-facies IF.

In apparent contrast to the Archean record, IF deposited in the middle to late Paleoproterozoic (ca. 2.3 Ga to 1.85 Ga) yielded $\delta^{56}Fe$ values ranging from $-0.66\permil$ to $1.1\permil$, with an average $\delta^{56}Fe$ value of $0.03\permil$ ($n = 19$). These samples are from cratonic settings and deep-water hydrothermal jaspers. The ca. 1.88 Ga IF have on average slightly more positive $\delta^{56}Fe$ values (e.g., Planavsky et al., 2009). IF and jaspers deposited in the Mesoproterozoic, Neoproterozoic, and Phanerozoic show $\delta^{56}Fe$ values ranging from $-0.87\permil$ to $1.66\permil$, with an average $\delta^{56}Fe$ value of $0.1\permil$ ($n = 28$). This group of iron-rich units consists largely of distal hydrothermal deposits but also includes IF associated with the 'Snowball Earth' glacial events (Supplementary Table 2).

5. DISCUSSION

5.1. Iron-formation depositional processes

Iron isotopes provide evidence that Fe enrichment in IF is predominantly caused by a deposition of Fe-oxides and
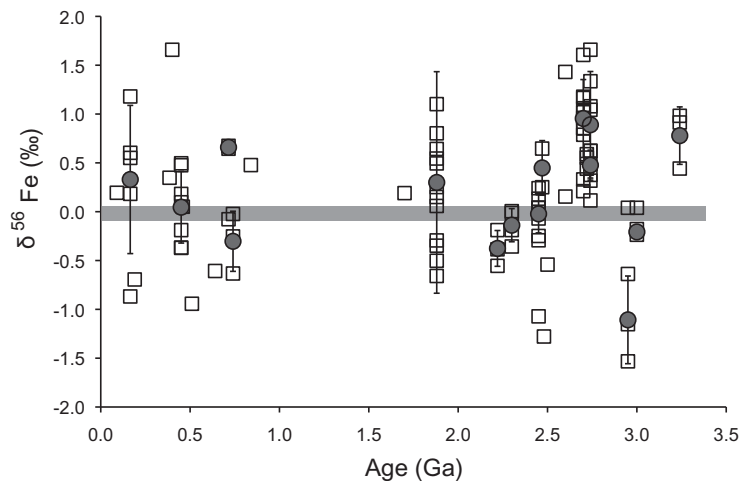
Fig. 1. Secular trend of whole-rock δ^{56}Fe values for iron formations. The open squares represent individual data points. The gray circles represent averages for formations for which several samples were analyzed and the black lines extending from the gray circles mark two standard deviations. The data for the ca. 1.88 Ga Animikie IF are a combination of new results and data from Planavsky et al. (2009).

Fe-oxyhydroxides. There is positive Fe isotope fractionation during microbial and abiotic Fe oxidation with a maximum fractionation of $\sim$2–3‰ (Bullen et al., 2001; Welch et al., 2003; Croal et al., 2004; Balci et al., 2006). This enrichment in heavy Fe isotopes contrasts with the isotope fractionations associated with siderite, ankerite, and green rust deposition, which are depleted in the heavy isotope relative to the ambient $Fe(II)_{aq}$ pool (Wiesli et al., 2004). Our bulk Fe isotope data are likely to reflect marine sedimentary and diagenetic processes, as we avoided samples that have been strongly influenced by ore-forming processes. Furthermore, late-stage, post-depositional (metamorphic) mineral transformations in IF determine Fe isotope composition of secondary minerals but not the whole rock (e.g., Frost et al., 2007). Fe repartitioning among minerals occurs in a closed system at our scale of observation. Therefore, predominantly positive δ^{56}Fe values in IF can be a signal of ferrous iron oxidation in the marine water column (Dauphas et al., 2004). This model builds on strong evidence that Fe in IF was derived from a seawater-dissolved pool, which was initially supplied from a hydrothermal source (Isley, 1995; Bau et al., 1997; Krapež et al., 2003; Beukes and Gutzmer, 2008) and therefore had a near crustal or negative δ^{56}Fe value (Severmann et al., 2004; Dauphas and Rouxel, 2006; Johnson et al., 2008a). This framework implies that the preserved mineral assemblage did not precipitate in isotopic equilibrium with the ancient oceans in cases where IF are dominated by reduced or mixed valence Fe mineral phases but positive bulk δ^{56}Fe values (see Johnson et al., 2008b). The reduced and mixed valence IF minerals (e.g., magnetite, siderite, and greenalite) therefore must have formed largely during early to late diagenesis or metamorphism, likely by nearly quantitative reduction of Fe oxides with positive δ^{56}Fe values (Johnson et al., 2008a; Steinhoefel et al., 2009; Craddock and Dauphas, 2011). This interpretation for the origin of siderite and magnetite in IF is fully consistent with previous detailed petrographic and carbon isotope data

(e.g., Ahn and Buseck, 1990; Kaufman et al., 1990; Pecoits et al., 2009) and is also consistent with some interpretations of the fine-scale Fe isotope variations in IF (e.g., Johnson et al., 2008a,b; Craddock and Dauphas, 2011).

The presence of positive δ^{56}Fe values in bulk IF likely points to low oxidizing potential in basins where the IF were deposited. Rather than showing positive Fe isotope values, bulk rock Fe-oxides should record the δ^{56}Fe value of initial dissolved iron when there is near-quantitative oxidation. For example, plume fallout deposits near the Rainbow hydrothermal vent along the Mid-Atlantic Ridge are generally similar in their δ^{56}Fe values to vent fluids due to quantitative Fe oxidation in oxic seawater (Severmann et al., 2004). Since IF are also chemically precipitated sediments with the Fe derived from hydrothermal fluids, modern submarine hydrothermal plume deposits provide useful analogs, as they also lack sulfide minerals and appreciable organic C enrichment. In contrast to what we observe, the variably negative δ^{56}Fe values in Late Cenozoic hydrogeneous crusts, although not fully understood, likely reflect quantitative precipitation of oceanic Fe derived from diverse sources, such as atmospheric input, shelf-derived Fe, and hydrothermal sources (Severmann et al., 2006, 2008; Staubwasser et al., 2006; Anbar and Rouxel, 2007; Rouxel et al., 2008b). Complex interactions with organic ligands in the water column may also contribute to the δ^{56}Fe variations. As previously discussed in Rouxel et al. (2003), both positive and negative δ^{56}Fe values in Phanerozoic Fe-rich hydrothermal cherts are likely the result of partial oxidation near or below the seafloor during the circulation of low-temperature hydrothermal fluids through volcanics on the ocean floor. In all cases, incomplete oxidation is required for the expression of the Fe-oxide Fe isotope fractionation and requires low oxygen or anoxic conditions. It follows that the δ^{56}Fe values of bulk samples of IF are likely to be strongly influenced by the extent of oxidation (Dauphas and Rouxel, 2006; Planavsky et al., 2009; Steinhoefel et al., 2009).
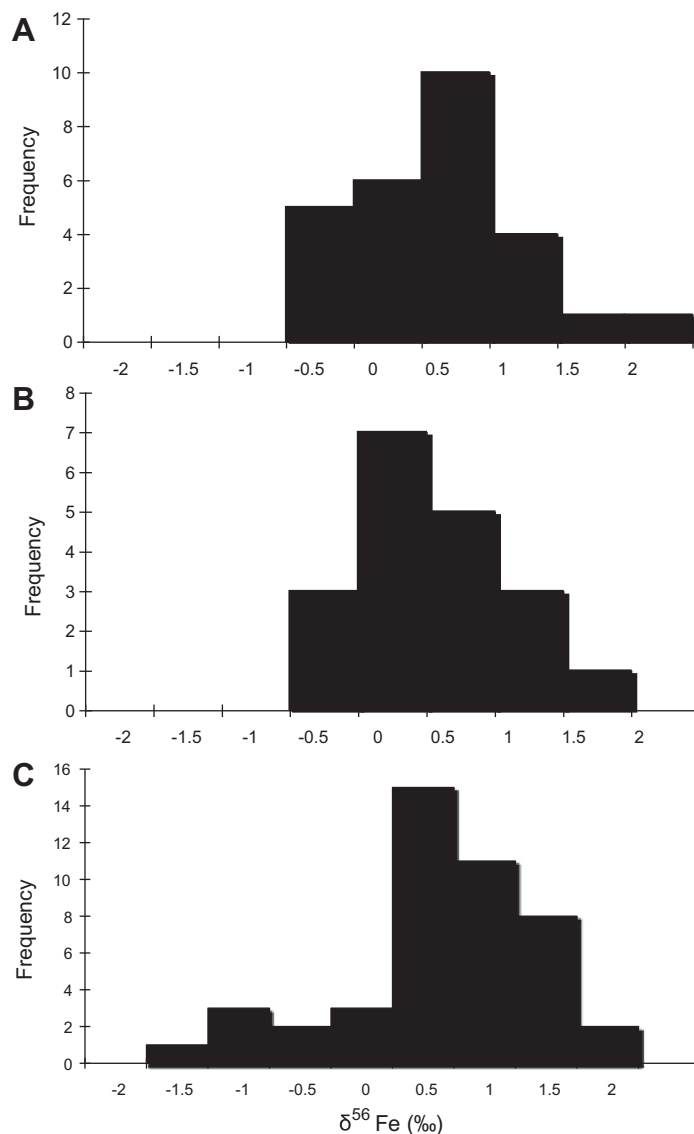
Fig. 2. Histograms of whole-rock $\delta^{56}Fe$ values for iron formations (A) Mesoproterozoic, Neoproterozoic, and Phanerozoic iron formations (0.1‰ average). (B) IF ranging in age from ca. 2.32 to ca. 1.88 Ga (0.0‰ average). (C) Samples with ages ranging from ca. 3.0 to ca. 2.4 Ga. The IF deposited before the rise of atmospheric oxygen at ca. 2.4 Ga (Bekker et al., 2004) have predominantly positive iron isotope values (0.4‰ average). The data for the ca. 1.88 Ga IF are a combination of new results and data from Planavsky et al. (2009).

The REE compositions of the same IF samples examined in this study for their Fe properties provide strong support for the partial oxidation model (cf. Planavsky et al., 2010). IF deposited before ca. 2.4 Ga show no deviation from trivalent Ce behavior, suggesting that the water column from which ferric oxides and oxyhydroxides precipitated was reducing with respect to manganese (cf. Bau and Dulski, 1996). There is also a shift in the variation in trivalent REE behavior in IF deposited before and after the rise of atmospheric oxygen. Archean and early Paleoproterozoic IF are characterized by consistent depletion in light REE and high Y/Ho ratios. These features contrast markedly with late Paleoproterozoic IF, which show significant ranges in light-to-heavy REE ($Pr/Yb_{(SN)}$) and Y/Ho ratios both below and above the reference value of the shale composite. The range of light-to-heavy REE and Y/Ho ratios in late Paleoproterozoic IF likely reflects varying impacts from Mn- and Fe-oxyhydroxide precipitation/dissolution. This interpretation implies deposition of late Paleoproterozoic (ca. 1.88 Ga) IF in basins with widely varying redox conditions. A dynamic redoxcline must have separated the oxic upper part of the water column from the suboxic to anoxic deeper parts in the late Paleoproterozoic, but this redox stratification was rare or absent in Archean basins (Planavsky et al., 2010).

Alternatively, positive $\delta^{56}Fe$ values in IF may reflect extensive re-reduction and release of isotopically light Fe following near-quantitative rather than partial Fe oxidation (Johnson et al., 2008a). Since DIR has been proposed to preferentially release light Fe isotopes to solution (e.g.,

Beard et al., 1999), partial reduction within the sediments of ferric oxides that rained down through the water column would leave residual oxides with positive δ^{56}Fe values. However, it is unlikely that DIR would have had a major influence on the Fe isotope composition of bulk sediments in extremely organic matter-poor, oxide-dominated IF, since the flux of reactive iron oxides was much greater than the input of organic matter. Additionally, even though DIR can be highly efficient, it is likely that only a small portion of Fe(II) would be lost back to the water column, with a larger fraction being absorbed onto Fe(III) oxyhydroxides or precipitated as Fe carbonates or Fe silicates. Importantly, diagenetic precipitation of mixed valence Fe oxides should not significantly alter the whole-rock Fe isotope composition of IF.

The negative whole-rock δ^{56}Fe values in our Archean and Paleoproterozoic IF samples, although relatively rare (<20% of the dataset), likely provide additional insight into the early Fe cycle. Early diagenetic Fe cycling in low sulfate environments creates two Fe reservoirs: one mobile and isotopically light and the other immobile and isotopically heavy. As discussed above, unless there is a net loss into the overlying water column of isotopically light Fe by diffusion through the sediment, bulk sediment values should not be affected by microbial reduction of the Fe(III) load. Accordingly, negative values of the bulk samples of IF indicate a particulate flux of isotopically light Fe to the sediments.

There are two commonly proposed models for fluxes of isotopically negative Fe to sediments from the overlying water column, and both could have contributed to the origin of IF with negative whole-rock δ^{56}Fe values. The flux of light Fe could be the result of near-quantitative oxidation in the water column of DIR products (e.g., Severmann et al., 2008). Second, Rayleigh-type fractionation during partial Fe(II) oxidation could create an isotopically light reservoir of residual dissolve Fe that is transferred to the sediment pile with later oxidation (e.g., Rouxel et al., 2005; Steinhoefel et al., 2009; Tsikos et al., 2010). Importantly, in both models, negative whole-rock δ^{56}Fe signatures likely reflect temporal or spatial variation in seawater δ^{56}Fe values.

In the Rayleigh fractionation model, the isotopically light Fe would be sourced from hydrothermal systems, with the dissolved Fe experiencing partial oxidation during transport from hydrothermal centers to shallower depositional settings (cf., von Blanckenburg et al., 2008). Partial oxidation could also occur in a hydrothermal plume with little vertical movement. Oxidation would result in a greater enrichment in the lighter Fe isotopes in the remaining dissolved Fe pool. A possibility is that anoxygenic phototropic oxidation could establish significant water column Fe concentration gradients – and therefore Fe isotope gradients – through ferric Fe removal during upwelling. This model is consistent with the generally accepted genetic models for Archean and Paleoproterozoic IF – specifically, a hydrothermal Fe supply in combination with a water column Fe concentration gradient (Bau and Dulski, 1996; Sumner, 1997; Sumner and Grotzinger, 2004). The lack of evidence for a discrete (sharp) redoxcline based on the REE composition of the Archean shallow-water carbonates (Planavsky et al., 2010) is also consistent with this model.

Accordingly, the Fe isotope composition throughout the water column in the Archean oceans likely mimicked the isotope behavior of nutrient-type elements that show variations with depth in the modern ocean, such as Si (e.g., Reynolds et al., 2006).

Alternatively, the isotopically light Fe could have been supplied by a "benthic Fe shuttle" (Severmann et al., 2008). In this model DIR creates an isotopically light Fe pool in porewaters, which diffuses from the sediments and is transported to and eventually precipitated in the deeper portion of the basin. In modern redox-stratified basins (e.g., Black Sea), there is a flux of Fe from sediments on the oxic shelf into the deep, euxinic portion of the basin (e.g., Lyons and Severmann, 2006). Similar processes may have operated in Archean basins (Raiswell, 2006; Severmann et al., 2008). However, it is likely that in shallow stretches of the Archean oceans the relatively small flux Fe oxides was rapidly and quantitatively reduced in the upper part of the sediment pile. This would have limited isotopic expression of microbial Fe reduction and thus of the modern "benthic Fe shuttle". In the Archean, the shallow oceans, in contrast to the Fe oxide-rich deep oceans, were extremely oxidant limited – a redox structure coined the upside-down biosphere (Walker, 1984). Partial Fe reduction was more common in the deep oceans than on the continental shelves in the Archean (Walker, 1984).

5.2. Comparison with previous Fe isotope studies of IF

Our Fe isotope results for a broad survey of IF are consistent with several studies of Eoarchean (ca. 3.8 Ga) and Neoarchean (ca. 2.7 Ga) deposits (Dauphas et al., 2004; Rouxel et al., 2005; Steinhoefel et al., 2009), which also revealed predominantly positive iron isotope values. Johnson et al. (2008) concluded that IF in the Transvaal basin and Hamersley province (Beukes and Gutzmer, 2008) have an average bulk δ^{56}Fe value around 0‰, which they interpreted to represent the average composition of late Neoarchean and early Paleoproterozic IF. This 0‰ average value is significant because it is just slightly above the average Fe isotope value of hydrothermally derived Fe (Rouxel et al., 2003; Severmann et al., 2004), implying near-quantitative oxidation of dissolved iron in seawater. However, since the study by Johnson et al. (2008a) was based on samples from mineralogically pure siderite and magnetite microlaminae, the data should be viewed with some caution. Specifically, this sampling strategy has a potential to skew the data toward negative values (relative to the bulk samples), since these microlaminae might be linked to Fe derived from microbial Fe reduction (Johnson et al., 2008a). A subsequent study found that the Brockman Iron Formation in the Hamersley province has slightly positive average δ^{56}Fe values (Craddock and Dauphas, 2011).

Further work is needed to explore whether there was a temporal change in the Fe isotope composition of IF prior to the rise of atmospheric oxygen. Although an extensive dataset is already available for Late Archean and early Paleoproterozoic IF (e.g., Johnson et al., 2008a; Heimann et al., 2010), additional data including whole-rock analyses would test the idea that Late Archean IFs have a near-crustal iron

isotope composition. Further, although our study is a step forward in establishing the whole-rock Fe isotope composition of diverse Archean IF, it should be regarded as preliminary given the number and diversity of Archean IF.

Tsikos et al. (2010) recently interpreted markedly negative Fe isotope values in the Fe- and Mn-rich Hotazel Formation in South Africa to be the result of Rayleigh distillation and deposition of isotopically heavy Fe oxide-rich rocks. This is consistent with our interpretation that the negative values in bulk samples of IF likely reflect dissolved marine Fe isotope compositions.

5.3. Iron isotope mass balance in the Earth's early oceans

Since our study suggests that IF older than ca. 2.4 Ga are a sink for isotopically heavy Fe, there must be a corresponding contemporaneous sink of isotopically light Fe in the sedimentary record. Pyritic black shale and, to a lesser extent, carbonates appear to be at least part of this sink (Fig. 3). Bulk samples of Archean black shales and sedimentary pyrites are characterized by persistently and anomalously low $\delta^{56}Fe$ values (Rouxel et al., 2005, 2006; Yamaguchi et al., 2005). Carbonates of this age also have highly negative $\delta^{56}Fe$ values (von Blanckenburg et al., 2008; Czaja et al., 2010). As discussed above, bulk IF can also be sinks of isotopically light Fe. The origin of these highly negative $\delta^{56}Fe$ values in sedimentary pyrite and carbonates has been heavily debated. For example, they have been linked to a period of extensive DIR in a low sulfate ocean at the end of the Archean (e.g., Johnson et al., 2008a; Heimann et al., 2010). However, large Fe isotope fractionations have not been observed during DIR in modern sulfate-poor aquatic systems (e.g., Teutsch et al., 2009; Tangalos et al., 2010) – in conflict with this model. Guilbaud et al. (2011) suggested that the light Fe isotope values in Archean sedimentary rocks were linked to fractionation during pyrite formation. Instead, Rouxel et al. (2005) attributed these

values to deposition of isotopically heavy, Fe oxide-rich IF in the deep-water portions of basins, which left the residual dissolved pool light. Our results provide additional support for this model. Specifically, we confirm that many IFs have positive average $\delta^{56}Fe$ values.

In most reconstructions of Archean basins, black shales are inferred to have formed landward with respect to the deeper-water IF (Beukes and Gutzmer, 2008; Bekker et al., 2009; Reinhard et al., 2009). The black shales, which contain the lowest $\delta^{56}Fe$ values, often display evidence for formation in euxinic settings or near the interface between shallow euxinic and deeper ferruginous conditions (Scott et al., 2008; Bekker et al., 2009; Reinhard et al., 2009). By analogy with modern marine euxinic settings (e.g., Lyons, 1997) and modern ferruginous lakes (e.g., Bura-Naki et al., 2009), a large portion of the sulfides found in black shales likely formed in the water column. Thus, partial Fe oxidation that drove IF deposition would have left a pool of isotopically light dissolved iron that was transferred to the sedimentary record as pyrite. In this scenario, the negative Fe isotope values in Archean black shales are linked predominantly to ocean-scale removal of heavy Fe via Fe oxide phases.

An assumption in the above outlined model is that there is limited Fe isotope fractionation during pyrite formation, so that the observed negative $\delta^{56}Fe$ values for pyrite are an archive of an ocean pool of light dissolved Fe (Rouxel et al., 2005). This assumption is valid if the sulfides formed in sulfide-rich/Fe-limiting euxinic conditions, where there will be nearly quantitative Fe removal. The exact fractionation factor during pyrite formation in Fe-unlimited conditions is unclear. Based on theoretical calculation, it is likely that the equilibrium fractionation factor during pyrite formation is around $-1‰$ ($Fe[II]_{aq}$-mineral) (Polyakov et al., 2007). In contrast, there is evidence from experiments and observations in natural systems for significant positive ($Fe[II]_{aq}$-mineral) kinetic – and possibly equilibrium – isotope
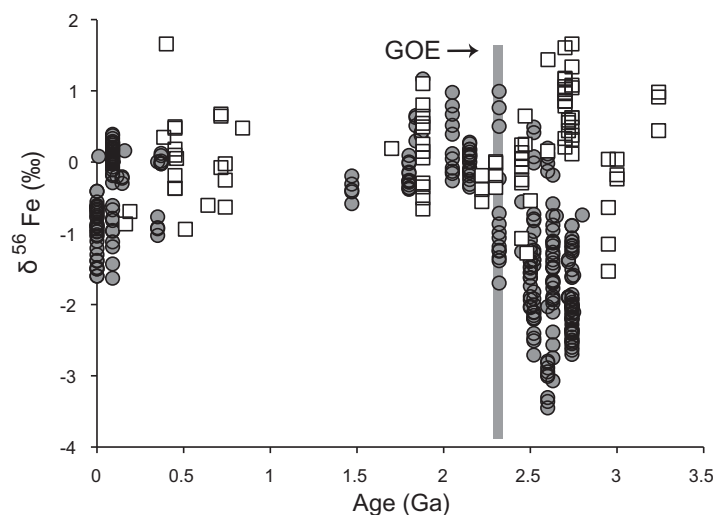

Fig. 3. Secular trend of whole-rock $\delta^{56}Fe$ values for iron formations from this study (empty squares) and $\delta^{56}Fe$ values for sedimentary pyrites (gray circles) from literature (Rouxel et al., 2005; Yamaguchi et al., 2005; Severmann et al., 2006; Clayton et al., 2007; Jenkyns et al., 2007; Fehr et al., 2008, 2010; Bekker et al., 2010). Gray vertical bar delineates the Great Oxidation Event (GOE).

fractionation during precipitation of 'FeS', a pyrite precursor (Butler et al., 2005), and pyrite (Guilbaud et al., 2011). The fractionation during FeS formation can be up to 0.9‰ in both hydrothermal and sedimentary settings and probably depends on the rate of FeS formation. There can also be a several per mil negative kinetic isotope fractionation during pyrite formation (Guilbaud et al., 2011). However, there is Fe isotope exchange and a progressive change towards isotopically heavy FeS on a relatively short (hourly) time scale – pushing the particulate sulfides heavy (Butler et al., 2005). Since large portion of the sulfide in modern Fe-rich aquatic systems is present as nanometer-scale aggregates (nanoparticles) of metal sulfide molecular clusters (Luther and Rickard, 2005), isotopic exchange is expected to be rapid while settling times to be very slow, which argues against a positive fractionation ($Fe[II]_{aq}$-mineral) during pyrite formation in anoxic aquatic systems. However, further Fe isotope work in modern Fe-rich aquatic systems is needed to better understand Fe isotope fractionation during sulfide formation.

Despite uncertainties about Fe isotope fractionation during pyrite formation in ferruginous conditions, available evidence points towards redox evolution as the origin for markedly light iron isotope values in the Archean. We propose that the markedly negative $\delta^{56}Fe$ values (down to $-3.5‰$) present in the Archean sedimentary pyrites, which are unknown in the Phanerozoic black shale geological record (Rouxel et al., 2005), reflect a time period when reducing marine conditions prevailed and yet significant iron oxidation occurred in the water column. This combination would have allowed for separation and burial of isotopically distinct pools of Fe as facilitated by partial Fe oxidation even when the size of the marine dissolved iron reservoir was diminished. Precipitation of around half of an initial hydrothermal Fe pool as isotopically heavy Fe oxides is needed for formation of sulfides with $\delta^{56}Fe$ values of -1.5 to $-2.0‰$ that are typical of Late Archean sulfides. The partial oxidation model requires that more than 90% of Fe is removed by precipitation of Fe oxides to explain the most negative iron isotope values as low as $-3.5‰$ (Rouxel et al., 2005). This level of iron drawdown is consistent with geologic and petrographic evidence for a large water column Fe concentration gradient and μM levels of iron even in the mixed layer of the Archean ocean (Sumner, 1997). Further, given Fe oxidation rates typical of modern anoxygenic photosynthesizers, a simple box model suggests variable extents of Fe oxidation during upwelling using the observed range of upwelling rates in the modern ocean. There is even the potential for quantitative oxidation despite high initial dissolved Fe concentrations (Kappler et al., 2005). Therefore, there are likely have been water column Fe isotope gradients in the Archean ocean.

In a reducing ocean, Fe emanating from hydrothermal centers could undergo partial oxidation in the upper water column by anoxic oxidation (e.g., anoxygenic photosynthetic Fe oxidation) or microaerophilic oxidation during plume transport. Partial oxidation would produce Fe-rich sediments with positive $\delta^{56}Fe$ values – as we observe in our bulk samples. If the matured plume/water parcel entered the sulfidic zone in shallower waters (likely on continental shelves),

sulfides with negative $\delta^{56}Fe$ values would have precipitated (e.g., Bekker et al., 2009). This model is consistent with the presence of markedly negative Fe isotope values in shales independently determined to be deposited under euxinic (Fe limited) conditions (Rouxel et al., 2005; Scott et al., 2008, 2011; Reinhard et al., 2009). In contrast, with a high surface-water oxidizing potential, the zone of partial Fe oxidation would condense, resulting in limited expression of Rayleigh isotope fractionation due to quantitative oxidation (Fig. 4).

Oxidative removal of dissolved Fe could have facilitated the formation of sulfidic water masses; removal of Fe oxides would increase the SO_4^{2-}/Fe^{2+} ratio in the water column, favoring euxinia. Oxide burial would dominate over pyrite burial if there was a limited sulfate supply or when there was a limited organic matter flux to fuel sulfate reduction. Since organic productivity varies greatly within oceans, the redox chemistry of a water mass would likely change along a circulation path. This model provides a simple explanation for why organic matter-rich shales deposited under euxinic conditions, a sedimentary rock type relatively common throughout the Earth's history, would have unusually negative Fe isotope values prior to the Great Oxidation Event (Figs. 3 and 4).

6. CONCLUSIONS

New whole-rock Fe isotope data for IF and other iron-rich sedimentary rocks indicate that Archean and early Paleoproterozoic IF were a sink for isotopically heavy Fe, in contrast to the later Proterozoic and Phanerozoic iron oxide-rich rocks. The positive $\delta^{56}Fe$ values indicate that IF deposition in the Archean was linked with a rain of ferric oxides and oxyhydroxides to the sediment–water interface. Positive Fe isotope values are likely linked to Fe isotope fractionation associated with partial ferrous Fe oxidation under Fe-replete conditions. These fractionations, in contrast, are muted by near-complete oxidation in younger deposits. The prevalence of partial oxidation is consistent with other evidence for a diffuse rather than sharp redoxcline and generally reducing conditions in the Archean oceans (Bau and Dulski, 1996; Sumner, 1997; Alexander et al., 2008; Planavsky et al., 2010).

Since our study suggests that IF are a sink for isotopically heavy Fe, there must be a corresponding reservoir of isotopically light Fe in the sedimentary record. Pyrite in black shales appear to be part of this sink. The persistently and anomalously low $\delta^{56}Fe$ values seen in these rocks (Rouxel et al., 2005; Yamaguchi et al., 2005) can be linked with deposition of isotopically heavy Fe in the deeper parts of basins and the transport of Fe with negative $\delta^{56}Fe$ values to shallower, more shoreward settings where shale deposition and abundant pyrite formation occurred.

Archean black shales with notably low and variable Fe isotope values are typically inferred to have formed landward of the deeper-water IF, and often in a sulfidic zone (Bekker et al., 2009; Reinhard et al., 2009; Scott et al., 2011). The markedly negative $\delta^{56}Fe$ values of the Archean sedimentary pyrite could reflect a time when reducing marine conditions prevailed. This redox state would have allowed
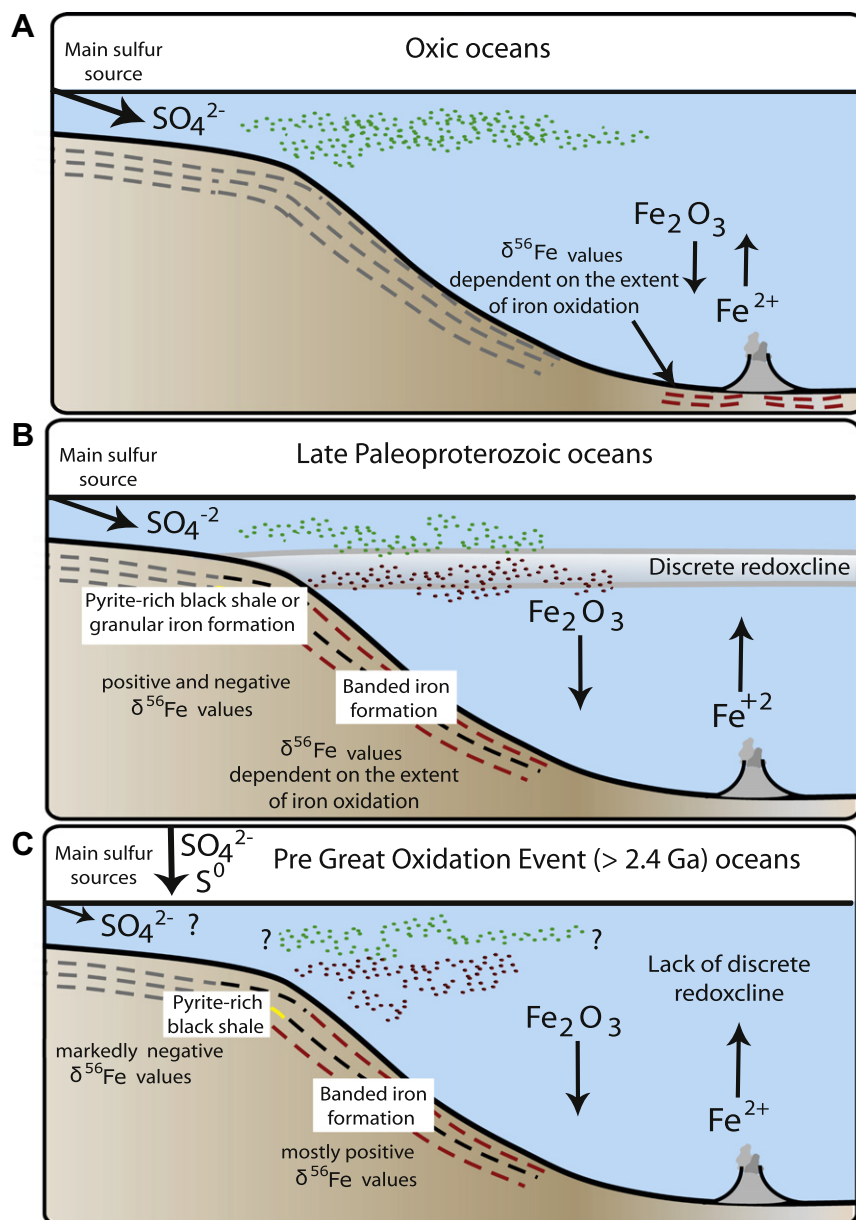
Fig. 4. (A) Iron has a short residence time in the modern oxidized open ocean; a redoxcline is lacking. (B) In the late Paleoproterozoic (ca. 1.88 Ga) ocean, Fe had a longer residence time and was deposited forming Fe formations at a discrete redoxcline separating anoxic to suboxic deep-waters and oxic shallow-waters. Above and at the redoxcline, Fe was deposited with granular iron formations and pyrite-rich black shales. (C) Model explaining the presence of markedly negative $\delta^{56}Fe$ values in pre-GOE black shales and sedimentary pyrites. Partial ferrous Fe oxidation led to deposition of iron formations and other iron-rich sediments with positive $\delta^{56}Fe$ values in the deeper water part of the ocean. This gave rise to an isotopically light pool of iron, which precipitated as Fe sulfides or Fe carbonates on the shelf and upper slope. A diffuse rather than a sharp redoxcline was present in the oceans at that time.

for separation and burial of isotopically distinct pools of Fe as well as for partial oxidation even as the size of dissolved Fe pool decreased by ferric oxide and oxyhydroxide deposition. At times with higher surface-water oxidation potential, the zone of partial iron oxidation would have shrunk, resulting in limited expression of the fractionation associated with Fe oxidation since Fe removal under these conditions would be quantitative. Thus, the Fe isotope records of marine shales and IF, when viewed together, capture the redox evolution of the oceans and suggest that the Archean and early Paleoproterozoic oceans before the rise of atmospheric oxygen typically lacked a sharp, persistent, and pervasive redoxcline, consistent with independent arguments based on REE systematics (e.g., Planavsky et al., 2010).

APPENDIX A. SUPPLEMENTARY DATA

Supplementary data associated with this article can be found, in the online version, at doi:10.1016/j.gca.2011.12. 001.

REFERENCES

Ahn J. H. and Buseck P. R. (1990) Hematite nanospheres of possible colloidal origin from a Precambrian banded iron formation. *Nature* **250**, 111–113.

Alexander B. W., Bau M., Andersson P. and Dulski P. (2008) Continentally-derived solutes in shallow Archean seawater: rare earth element and Nd isotope evidence in iron formation from the 2.9 Ga Pongola Supergroup, South Africa. *Geochim. Cosmochim. Acta* **72**, 378–394.

Anbar A. D. and Rouxel O. (2007) Metal stable isotopes in paleoceanography. *Annu. Rev. Earth Planet. Sci.* **35**, 717–746.

Anbar A. D., Jarzecki A. A. and Spiro T. G. (2005) Theoretical investigation of iron isotope fractionation between $Fe(H_2O)(3+)(6)$ and $Fe(H_2O)(2+)(6)$: implications for iron stable isotope geochemistry. *Geochim. Cosmochim. Acta* **69**, 825–837.

Balci N., Bullen T. D., Witte-Lien K., Shanks W. C., Motelica M. and Mandernack K. W. (2006) Iron isotope fractionation during microbially stimulated Fe(II) oxidation and Fe(III) precipitation. *Geochim. Cosmochim. Acta* **70**, 622–639.

Bau M. and Dulski P. (1996) Distribution of yttrium and rare-earth elements in the Penge and Kuruman iron-formations, Transvaal Supergroup, South Africa. *Precambrian Res.* **79**, 37–55.

Bau M., Hohndorf A., Dulski P. and Beukes N. J. (1997) Sources of rare-earth elements and iron in paleoproterozoic iron-formations from the Transvaal Supergroup, South Africa: evidence from neodymium isotopes. *J. Geol.* **105**, 121–129.

Beard B. L., Johnson C. M., Cox L., Sun H., Nealson K. H. and Aguilar C. (1999) Iron isotope biosignatures. *Science* **285**, 1889–1892.

Beard B. L., Johnson C. M., Skulan J. L., Nealson K. H., Cox L. and Sun H. (2003) Application of Fe isotopes to tracing the geochemical and biological cycling of Fe, Special issue on Isotopic Record of Microbially Mediated Processes. *Chem. Geol.* **195**, 87–117.

Beard B., Handler R., Scherer M., Wu L., Czaja A., Heimann A. and Johnson C. (2010) Iron isotope fractionation between aqueous ferrous iron and goethite. *Earth Planet. Sci. Lett.* **295**, 241–250.

Bekker A., Holland H. D., Wang P.-L., Rumble, III, D., Stein H. J., Hannah J. L., Coetzee L. L. and Beukes N. J. (2004) Dating the rise of atmospheric oxygen. *Nature* **427**, 117–120.

Bekker A., Barley M. E., Fiorentini M. L., Rouxel O. J., Rumble D. and Beresford S. W. (2009) Atmospheric sulfur in Archean komatiite-hosted nickel deposits. *Science* **326**, 1086–1089.

Bekker A., Slack J., Planavsky N., Krapež B., Hofmann A., Konhauser K. O. and Rouxel O. J. (2010) Iron formation: the sedimentary product of a complex interplay among mantle, tectonic, oceanic, and biospheric processes. *Econ. Geol.* **105**, 467–508.

Bennett S. A., Rouxel O., Schmidt K., Garbe-Schonberg D., Statham P. J. and German C. R. (2009) Iron isotope fractionation in a buoyant hydrothermal plume, 5 degrees S Mid-Atlantic Ridge. *Geochim. Cosmochim. Acta* **73**, 5619–5634.

Bergquist B. A. and Boyle E. A. (2006) Iron isotopes in the Amazon River system: weathering and transport signatures. *Earth Planet. Sci. Lett.* **248**, 54–68.

Beukes N. J. and Gutzmer J. (2008) Origin and Paleoenvironmental significance of major iron formations at the Archean–Paleoproterozoic boundary. *Soc. Econ. Geol. Rev.* **15**, 5–47.

Bullen T. D., White A. F., Childs C. W., Vivit D. V. and Schulz M. S. (2001) Demonstration of significant abiotic iron isotope fractionation in nature. *Geology* **29**, 699–702.

Bura-Naki E., Viollier E., Jezequel D., Thiam A. and Ciglenecki I. (2009) Reduced sulfur and iron species in anoxic water column of meromictic crater Lake Pavin (Massif Central, France). *Chem. Geol.* **266**, 311–317.

Butler I. B., Archer C., Vance D., Oldroyd A. and Rickard D. (2005) Fe isotope fractionation on FeS formation in ambient aqueous solution. *Earth Planet. Sci. Lett.* **236**, 430–442.

Canfield D. E. (2005) The early history of atmospheric oxygen: Homage to Robert A Garrels. *Annu. Rev. Earth Planet. Sci.* **33**, 1–36.

Clayton R. E., Nederbragt A. J., Malinovsky D., Andersson P. and Thurow J. (2007) Iron isotope geochemistry of mid-Cretaceous organic-rich sediments at Demerara Rise (ODP Leg 207). *Proc. NZ Ecol. Soc.* **207**, 1–14.

Craddock P. R. and Dauphas N. (2011) Iron and carbon isotope evidence for microbial iron respiration throughout the Archean. *Earth Planet. Sci. Lett.* **303**, 121–132.

Croal L. R., Johnson C. M., Beard B. L. and Newman D. K. (2004) Iron isotope fractionation by Fe(II)-oxidizing photoautotrophic bacteria. *Geochim. Cosmochim. Acta* **68**, 1227–1242.

Crosby H. A., Johnson C. M., Roden E. E. and Beard B. L. (2005) Coupled Fe(II)-Fe(III) electron and atom exchange as a mechanism for Fe isotope fractionation during dissimilatory iron oxide reduction. *Environ. Sci. Technol.* **39**, 6698–6704.

Crosby H. A., Roden E. E., Johnson C. M. and Beard B. L. (2007) The mechanisms of iron isotope fractionation produced during dissimilatory Fe(III) reduction by *Shewanella putrefaciens* and *Geobacter sulfurreducens*. *Geobiology* **5**, 169–189.

Crowe S. A., Jones C., Katsev S., Magen C., O'Neill A. H., Sturm A., Canfield D. E., Haffner G. D., Mucci A., Sundby B. and Fowle D. A. (2008) Photoferrotrophs thrive in an Archean Ocean analogue. *Proc. Natl. Acad. Sci.* **105**, 15938–15943.

Czaja A., Johnson C., Beard B., Eigenbrode J., Freeman K. and Yamaguchi K. (2010) Iron and carbon isotope evidence for ecosystem and environmental diversity in the 2.7 to 2.5 Ga Hamersley Province, Western Australia. *Earth Planet. Sci. Lett.* **292**, 170–180.

Dauphas N. and Rouxel O. (2006) Mass spectrometry and natural variations of iron isotopes. *Mass Spectrom. Rev.* **25**, 515–550.

Dauphas N., van Zuilen M., Wadhwa M., Davis A. M., Marty B. and Janney P. E. (2004) Clues from iron isotope variations on

the origin of early Archaean banded iron formations from Greenland. *Science* **306**, 2077–2080.

Escoube R., Rouxel O. J., Sholkovitz E. and Donard O. F. X. (2009) Iron isotope systematics in estuaries: the case of North River, Massachusetts (USA). *Geochim. Cosmochim. Acta* **73**, 4045–4059.

Fehr M. A., Andersson P. S., Hålenius U. and Morth C.-M. (2008) Iron isotope variations in Holocene sediments of the Gotland Deep Baltic Sea. *Geochim. Cosmochim. Acta* **72**, 807–826.

Fehr M. A., Andersson P. S., Hålenius U., Gustafsson O. and Morth C.-M. (2010) Iron enrichments and Fe isotopic compositions of surface sediments from the Gotland Deep Baltic Sea. *Chem. Geol.* **277**, 310–322.

Frost C. D., von Blanckenburg F., Schoenberg R., Frost B. R. and Swapp S. M. (2007) Preservation of Fe isotope heterogeneities during diagenesis and metamorphism of banded iron formation. *Contrib. Mineral. Petr.* **153**, 211–235.

Gross G. (1980) A classification of iron-formation based on depositional environments. *Can. Mineral.* **18**, 223–229.

Guilbaud R., Butler I. B. and Ellam R. M. (2011) Abiotic pyrite formation produces a large Fe isotope fractionation. *Science* **332**, 1548–1551.

Hartman H. (1984) The evolution of photosynthesis and microbial mats: a speculation on the banded iron formations. In *Microbial Mats: Stromatolites* (eds. Y. Cohen, R. W. Castenholz and H. O. Halvorson). Alan R. Liss, New York, pp. 449–453.

Heimann A., Johnson C., Beard B., Valley J., Roden E., Spicuzza M. and Beukes N. (2010) Fe, C, and O isotope compositions of banded iron formation carbonates demonstrate a major role for dissimilatory iron reduction in 2.5 Ga marine environments. *Earth Planet. Sci. Lett.* **294**, 8–18.

Holland H. D. (2005) Sedimentary mineral deposits and the evolution of earth's near-surface environments. *Econ. Geol.* **100**, 1489–1509.

Homoky W. B., Severmann S., Mills R. A., Statham P. J. and Fones G. R. (2009) Pore-fluid Fe isotopes reflect the extent of benthic Fe redox recycling: evidence from continental shelf and deep-sea sediments. *Geology* **37**, 751–754.

Icopini G. A., Anbar A. D., Ruebush S. R., Tien M. and Brantley S. L. (2004) Iron isotope fractionation during microbial reduction of iron. *Geology* **32**, 205–208.

Isley A. E. (1995) Hydrothermal plumes and the delivery of iron to banded iron-formation. *J. Geol.* **103**, 169–185.

Jenkyns H. C., Matthews A., Tsikos H. and Erel Y. (2007) Nitrate reduction, sulfate reduction, and sedimentary iron isotope evolution during the Cenomanian–Turonian oceanic anoxic event. *Paleoceanography* **22**. doi:10.1029/2006PA001355.

John S. G. and Adkins J. F. (2010) Analysis of dissolved iron isotopes in seawater. *Mar. Chem.* **119**, 65–76.

Johnson C. M. and Beard B. (2006) Fe isotopes: an emerging technique in understanding modern and ancient biogeochemical cycles. *GSA Today* **16**, 4–10.

Johnson C. M., Beard B. L., Beukes N. J., Klein C. and O'Leary J. M. (2003) Ancient geochemical cycling in the Earth as inferred from Fe isotope studies of banded iron formations from the Transvaal Craton. *Contrib. Mineral. Petrol.* **144**, 523–547.

Johnson C. M., Beard B. L., Klein C., Beukes N. J. and Roden E. E. (2008a) Iron isotopes constrain biologic and abiologic processes in banded iron formation genesis. *Geochim. Cosmochim. Acta* **72**, 151–169.

Johnson C. M., Beard B. L. and Roden E. E. (2008b) The iron isotope fingerprints of redox and biogeochemical cycling in the modern and ancient Earth. *Annu. Rev. Earth Planet. Sci.* **36**, 457–493.

Kappler A., Pasquero C., Konhauser K. O. and Newman D. K. (2005) Deposition of banded iron formations by anoxygenic phototrophic Fe(II)-oxidizing bacteria. *Geology* **33**, 865–868.

Kaufman A. J., Hayes J. M. and Klein C. (1990) Primary and diagenetic controls of isotopic compositions of iron-formation carbonates. *Geochim. Cosmochim. Acta* **54**, 3461–3473.

Klein C. (2005) Some precambrian banded iron-formations (BIFs) from around the world: their age, geologic setting, mineralogy, metamorphism, geochemistry, and origin. *Am. Mineral.* **90**, 1473–1499.

Konhauser K. O., Hamade T., Raiswell R., Morris R. C., Ferris F. G., Southam G. and Canfield D. E. (2002) Could bacteria have formed the precambrian banded iron formations? *Geology* **30**, 1079–1082.

Krapež B., Barley M. E. and Pickard A. L. (2003) Hydrothermal and resedimented origins of the precursor sediments to banded iron formation: sedimentological evidence from the early palaeoproterozoic Brockman supersequence of Western Australia. *Sedimentology* **50**, 979–1011.

Lacan F., Radic A., Jeandel C., Poitrasson F., Sarthou G., Pradoux C. and Freydier R. (2008) Measurement of the isotopic composition of dissolved iron in the open ocean. *Geophys. Res. Lett.* **35**. doi:10.1029/2008GL035841.

Levasseur S., Frank M., Hein J. R. and Halliday A. N. (2004) The global variation in the iron isotope composition of marine hydrogenetic ferromanganese deposits: implications for seawater chemistry? *Earth Planet. Sci. Lett.* **224**, 91–105.

Luther G. W. and Rickard D. T. (2005) Metal sulfide cluster complexes and their biogeochemical importance in the environment. *J. Nanopart. Res.* **7**, 389–407.

Lyons T. W. (1997) Sulfur isotopic trends and pathways of iron sulfide formation in upper holocene sediments of the anoxic Black Sea. *Geochim. Cosmochim. Acta* **61**, 3367–3382.

Lyons T. W. and Severmann S. (2006) A critical look at iron paleoredox proxies: new insights from modern euxinic marine basins. *Geochim. Cosmochim. Acta* **70**, 5698–5722.

Pecoits E., Gingras M. K., Barley M. E., Kappler A., Posth N. R. and Konhauser K. O. (2009) Petrography and geochemistry of the Dales Gorge banded iron formation: paragenetic sequence, source and implications for palaeo-ocean chemistry. *Precambrian Res.* **172**, 163–187.

Planavsky N. J., Rouxel O. J., Bekker A., Shapiro R., Fralick P. and Knudsen A. (2009) Iron-oxidizing microbial ecosystems thrived in late Paleoproterozoic redox-stratified oceans. *Earth Planet. Sci. Lett.* **286**, 230–242.

Planavsky N. J., Bekker A., Rouxel O. J., Knudsen A. and Lyons T. W. (2010) Rare earth element and yttrium compositions of Archean and Paleoproterozoic iron formations revisited: new perspectives on the significance and mechanisms of deposition. *Geochim. Cosmochim. Acta* **74**, 6387–6405.

Polyakov V. B., Clayton R. N., Horita J. and Mineev S. D. (2007) Equilibrium iron isotope fractionation factors of minerals: reevaluation from the data of nuclear inelastic resonant X-ray scattering and Mössbauer spectroscopy. *Geochim. Cosmochim. Acta* **71**, 3833–3846.

Raiswell R. (2006) An evaluation of diagenetic recycling as a source of iron for banded iron formations. In *Evolution of Early Earth's Atmosphere, Hydrosphere and Biosphere – Constraints from Ore Deposits* (eds. S. E. Kesler and H. Ohmoto). Geological Society of America, Boulder, pp. 228–238.

Reinhard C. T., Raiswell R., Scott C., Anbar A. D. and Lyons T. W. (2009) A Late Archean Sulfidic Sea stimulated by early oxidative weathering of the continents. *Science* **326**, 713–716.

Reynolds B. C., Frank M. and Halliday A. N. (2006) Silicon isotope fractionation during nutrient utilization in the North Pacific. *Earth Planet. Sci. Lett.* **244**, 431–443.

Rouxel O. J. and Auro M. (2010) Iron isotope variations in coastal seawater determined by Multicollector ICP-MS4. *Geostan. Geoanal. Res.* doi:10.1111/j.1751-908X.2010.00063.x.

Rouxel O. J., Dobbek N., Ludden J. and Fouquet Y. (2003) Iron isotope fractionation during oceanic crust alteration. *Chem. Geol.* **202**, 155–182.

Rouxel O. J., Bekker A. and Edwards K. J. (2005) Iron isotope constraints on the Archean and Paleoproterozoic ocean redox state. *Science* **307**, 1088–1091.

Rouxel O. J., Bekker A. and Edwards K. (2006) Response to comment on "Iron isotope constraints on the Archean and Paleo-Proterozoic ocean redox state" by Yamaguchi K and Ohmoto H. *Science* **311**, 177b.

Rouxel O. J., Shanks W. C., Bach W. and Edwards K. J. (2008a) Integrated Fe- and S-isotope study of seafloor hydrothermal vents at East Pacific rise 9–10 degrees N. *Chem. Geol.* **252**, 214–227.

Rouxel O. J., Sholkovitz E., Charette M. and Edwards K. J. (2008b) Iron isotope fractionation in subterranean estuaries. *Geochim. Cosmochim. Acta* **72**, 3413–3430.

Scott C., Lyons T. W., Shen Y., Poulton S. W., Chu X. and Anbar A. D. (2008) Tracing the stepwise oxygenation of the Proterozoic ocean. *Nature* **452**, 457–460.

Scott C., Bekker A., Reinhard C. R., Schnetger B., Krapež B., Rumble D. and Lyons T. W. (2011) Late Archean euxinic conditions before the rise of atmospheric. *Geology* **39**, 119–122.

Severmann S., Johnson C. M., Beard B. L., German C. R., Edmonds H. N., Chiba H. and Green D. R. H. (2004) The effect of plume processes on the Fe isotope composition of hydrothermally derived Fe in the deep ocean as inferred from the Rainbow vent site, Mid-Atlantic Ridge, 36 degrees 14′ N. *Earth Planet. Sci. Lett.* **225**, 63–76.

Severmann S., Johnson C. M., Beard B. L. and McManus J. (2006) The effect of early diagenesis on the Fe isotope compositions of porewaters and authigenic minerals in continental margin sediments. *Geochim. Cosmochim. Acta* **70**, 2006–2022.

Severmann S., Lyons T. W., Anbar A., McManus J. and Gordon G. (2008) Modern iron isotope perspective on the benthic iron shuttle and the redox evolution of ancient oceans. *Geology* **36**, 487–490.

Staubwasser M., von Blanckenburg F. and Schoenberg R. (2006) Iron isotopes in the early marine diagenetic iron cycle. *Geology* **34**, 629–632.

Steinhoefel G., Horn I. and von Blanckenburg F. (2009) Microscale tracing of Fe and Si isotope signatures in banded iron formation using femtosecond laser ablation. *Geochim. Cosmochim. Acta* **73**, 5343–5360.

Sumner D. Y. (1997) Carbonate precipitation and oxygen stratification in late Archean seawater as deduced from facies and stratigraphy of the Gamohaan and Frisco formations, Transvaal Supergroup, South Africa. *Am. J. Sci.* **297**, 455–487.

Sumner D. Y. and Grotzinger J. P. (2004) Implications for Neoarchaean ocean chemistry from primary carbonate mineralogy of the Campbellrand-Malmani Platform, South Africa. *Sedimentology* **51**, 1273–1299.

Tangalos G. E., Beard B. L., Johnson C. M., Alpers C. N., Shelobolina E. S., Xu H., Konishi H. and Roden E. E. (2010) Microbial production of isotopically light iron(II) in a modern chemically-precipitated sediment and implications for isotopic variations in ancient rocks. *Geobiology* **8**, 197–208.

Tompkins L. A. and Cowan D. R. (2001) Opaque mineralogy and magnetic properties of selected banded iron-formations, Hamersley Basin, Western Australia. *Aust. J. Earth Sci.* **48**, 427–437.

Teutsch N., Schmid M., Muller B., Halliday A. N., Burgmann H. and Wehrli B. (2009) Large iron isotope fractionation at the oxic-anoxic boundary in Lake Nyos. *Earth Planet. Sci. Lett.* **285**, 52–60.

Tsikos H., Matthews A., Erel Y. and Moore J. M. (2010) Iron isotopes constrain biogeochemical redox cycling of iron and manganese in a Palaeoproterozoic stratified basin. *Earth Planet. Sci. Lett.* **298**, 125–134.

von Blanckenburg F., Marnberti M., Schoenberg R., Kamber B. S. and Webb G. E. (2008) The iron isotope composition of microbial carbonate. *Chem. Geol.* **249**, 113–128.

Walker J. C. G. (1984) Suboxic diagenesis in banded iron formations. *Nature* **309**, 340–342.

Welch S. A., Beard B. L., Johnson C. M. and Braterman P. S. (2003) Equilibrium Fe isotope fractionation between ferrous and ferric iron. *Geochim. Cosmochim. Acta* **67**, A529.

Widdel F., Schnell S., Heising S., Ehrenreich A., Assmus B. and Schink B. (1993) Ferrous iron oxidation by anoxygenic phototrophic bacteria. *Nature* **362**, 834–836.

Wiesli R. A., Beard B. L. and Johnson C. M. (2004) Experimental determination of Fe isotope fractionation between aqueous Fe(II), siderite and "green rust" in abiotic systems. *Chem. Geol.* **211**, 343–362.

Yamaguchi K. E., Johnson C. M., Beard B. L. and Ohmoto H. (2005) Biogeochemical cycling of iron in the Archean–Paleoproterozoic Earth: constraints from iron isotope variations in sedimentary rocks from the Kaapvaal and Pilbara Cratons. *Chem. Geol.* **218**, 135–169.

Associate editor: James Farquhar